

# Design, Synthesis, and Bioactivity of Novel Coumarin-3-carboxylic Acid Derivatives Containing a Thioether Quinoline Moiety

Yuanquan Zhang,<sup>§</sup> Zhiyuan Xu,<sup>§</sup> Minxiang Dou,<sup>§</sup> Yan Xu, Xin Fu, Fadi Zhu, Huochun Ye, Jing Zhang,\* and Gang Feng\*



Cite This: *ACS Omega* 2024, 9, 50695–50704



Read Online

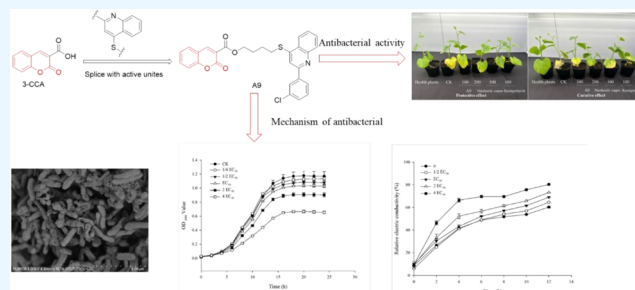
ACCESS |

Metrics & More

Article Recommendations

Supporting Information

**ABSTRACT:** A series of coumarin-3-carboxylic acid derivatives containing a thioether quinoline moiety were designed and synthesized. The structures of these compounds were determined using <sup>1</sup>H NMR, <sup>13</sup>C NMR, and HRMS. The antibacterial activity of the compounds was evaluated against *Xanthomonas oryzae* pv *oryzae* (*Xoo*), *Ralstonia solanacearum* (*Rs*), and *Acidovorax citrulli* (*Aac*). The results showed that most of the compounds exhibited significant antibacterial activity against these pathogens. Particularly, compound A9 demonstrated potent activity against *Xoo* and *Aac*, with EC<sub>50</sub> values of 11.05 and 8.05 μg/mL respectively. In addition, A9 indicated strong protective and curative effects against *Aac* *in vivo*, with efficacy rates of 61.50 and 54.86%, respectively, surpassing those of the positive control thiodiazole copper. The scanning electron microscopy observations revealed that treatment of *Aac* cells with A9 at a concentration of 2EC<sub>50</sub> resulted in a curved and sunken cell morphology, along with destroyed cell membrane integrity. Additionally, the motility and exopolysaccharide production of *Aac* were inhibited, and biofilm formation was prevented. Consequently, these newly developed derivatives of coumarin-3-carboxylic acid, incorporating the thioether quinoline moiety, hold promise as potential templates for the development of innovative antibacterial agents.



## 1. INTRODUCTION

Crop bacterial diseases caused by phytopathogenic bacteria pose significant challenges in terms of control due to their rapid spread, extensive range, and high resistance to pesticides.<sup>1</sup> Examples of such diseases include rice bacterial leaf blight caused by *Xanthomonas oryzae* pv *oryzae* (*Xoo*),<sup>2,3</sup> tomato bacterial wilt caused by *Ralstonia solanacearum* (*Rs*),<sup>4</sup> and melon bacterial fruit blotch caused by *Acidovorax citrulli* (*Aac*).<sup>5</sup> These diseases have a detrimental impact on crop growth, jeopardizing both the yield and quality. Currently, chemical control serves as the primary approach to managing bacterial diseases, predominantly relying on copper preparations and antibiotics. However, copper preparations exhibit limited efficacy and are susceptible to produce drug damage to crops,<sup>6</sup> while antibiotics are prone to induce antibiotic resistance and pollute the environment.<sup>7</sup> Consequently, there is a pressing need to develop a novel, ecofriendly bactericide that is both sustainable and environmentally benign for effective control of bacterial diseases.

Coumarin-3-carboxylic acid (3-CCA) is a naturally occurring derivative of coumarin that has been shown to possess antitumor properties,<sup>8</sup> as well as anticancer effects<sup>9–11</sup> and antimicrobial activities.<sup>12,13</sup> Previous investigations have demonstrated the broad-spectrum antibacterial activity of 3-CCA;<sup>14</sup> however, the precise structure–activity relationship

(SARs) remains incompletely understood. Prior research has indicated that structural modifications of 3-CCA can yield compounds with potent fungicidal,<sup>15</sup> antibacterial,<sup>16</sup> and antagonist properties.<sup>17</sup> It is anticipated that the enhancement of bactericidal activity can be achieved through the incorporation of diverse agricultural bactericidal active groups at the 3 sites.

Quinoline, a significant bioactive natural alkaloid, has garnered considerable interest in recent years due to its remarkable antifungal,<sup>18,19</sup> antimalaria,<sup>20</sup> antitumor,<sup>21–23</sup> antinucleation,<sup>24,25</sup> and other biological activities.<sup>26</sup> Consequently, it has emerged as a prominent lead compound for the development of novel pesticides. Notably, several quinoline-based compounds, including Quinoxifen, Quinclorac, and Tebufloquin have been successfully developed and introduced to the market.

In our previous work, the incorporation of thioether quinoline into the molecular framework of myricetin was

**Received:** September 23, 2024

**Revised:** November 19, 2024

**Accepted:** November 26, 2024

**Published:** December 11, 2024



achieved using active splicing methodology, resulting in the synthesis of myricetin derivative B6 featuring containing thioether quinoline moieties that exhibit a pronounced affinity toward TMV-P.<sup>27</sup> This finding suggests that thioether quinoline, when utilized as a pharmacophore, can augment the antiviral efficacy of the parent compound. Nevertheless, the structural characterization of 3-CCA compounds incorporating thioether quinoline groups remains unexplored in the literature.

In this study, the thioether quinoline was introduced into the structure of 3-CCA through active splicing. A total of thirty-eight derivatives of 3-CCA containing thioether quinoline were synthesized and evaluated for their antibacterial activities against *Xoo*, *Rs*, and *Aac* *in vitro*. The EC<sub>50</sub> values and *in vivo* efficacy of the most effective compound were determined. The effects of potent compounds on physiological and biochemical indicators of sensitive bacteria, such as bacterial morphology, motility, and cell membrane integrity, were also assessed. The results of this study may offer valuable insights into the development of novel antibacterial agents derived from coumarin compounds.

## 2. MATERIALS AND METHODS

### 2.1. Instruments and Chemicals. 2.1.1. Instruments.

The chemical reaction processes were monitored through thin-layer chromatography (TLC) under an ultraviolet lamp. The melting points of the compounds were determined by using a melting point apparatus (Shanghai INESA Optical Instrument Co., Ltd., China) without temperature calibration. The <sup>1</sup>H and <sup>13</sup>C NMR spectra were obtained using a Bruker DKX500 NMR spectrometer (Bruker; Karlsruhe, Germany) with CDCl<sub>3</sub> or DMSO-*d*<sub>6</sub> as the solvent and TMS as the internal standard. The Thermo Scientific Q Exactive (Thermo Scientific, Missouri, MO) instrument was utilized to obtain high-resolution mass spectrometry (HRMS) data of the compounds.

**2.1.2. Chemicals.** All chemical reagents utilized in this study were commercially available and were not subjected to further purification. The present study procured various reaction materials from Shanghai Titan Technology Co., Ltd. (Shanghai, China) and other chemical materials from Bositai Technology Co., Ltd. (Chongqing, China). Coumarin-3-carboxylic acid (3-CCA, 95%) was obtained from Bide Pharmatech Ltd. (Shanghai, China), while kasugamycin (65%) and a water solution (2%) were sourced from Shenzhen Novoxin Agrochemical Co., Ltd. (Shenzhen, China). All chemical reagents and solvents utilized in the study were of analytical purity.

**2.1.3. Bacteria.** In this study, three phytopathogenic bacterial strains assayed for *in vitro* antibacterial screening were *Xoo* (bacterial leaf blight of rice), *Aac* (bacterial fruit blotch), and *Rs* (tomato bacterial wilt). These strains were preserved for long-term use by storing them in 20% glycerol at -80 °C. The strains were cultured either on Luria-Bertani agar (LA) plates, which contained 10 g of tryptone, 5 g of yeast extract, 10 g of NaCl, 16 g of agar, and 1 L of distilled water, or in LB broth (without agar) at 28 °C in the dark.

**2.2. Synthesis. 2.2.1. General Synthetic Procedure for the Intermediate 1.**  $\alpha$ -Aminoacetophenone (150 mmol) and triethylamine (150 mmol) were added to 150 mL of anhydrous CH<sub>2</sub>Cl<sub>2</sub>. At 0 °C, various substitutes of benzoyl chloride (150 mmol) dissolved in 150 mL CH<sub>2</sub>Cl<sub>2</sub> was added dropwise. The reaction continued at room temperature for about 3 h after

dropping. The reaction was monitored by thin-layer chromatography (TLC) until it was completed. After the reaction was completed, an appropriate amount of water was added for washing. The organic phase was dried with anhydrous Na<sub>2</sub>SO<sub>4</sub>. After desolubilization, it was recrystallized with petroleum ether-ethyl acetate to obtain intermediate 1.<sup>28</sup>

**2.2.2. General Synthetic Procedure for the Intermediate 2.** Intermediate 1 (100 mmol) was added to 250 mL of 1,4-dioxane. NaOH (300 mmol) was added in batches; the temperature was slowly raised to 110 °C for 2 h. After the reaction was completed, the solvent was removed by the rotary evaporator. 300 mL of water was added to dissolve it, and then 1 mol/L HCl was used to adjust the solution pH to 7. After suction filtration, the filter cake was washed with water and dichloromethane-ethyl acetate mixed solution (v/v = 1:1) for several times to obtain intermediate 2.<sup>28</sup>

**2.2.3. General Synthetic Procedure for the Intermediate 3.** Intermediate 2 (90 mmol) was dissolved in 250 mL of anhydrous pyridine. Phosphorus pentasulfide (180 mmol) was slowly added at 0 °C, and the temperature was raised to 110 °C for 5 h. After the reaction was completed, the mixture was cooled to room temperature. A large amount of yellow precipitate appeared after adding an equal volume of water and stirring for a few minutes. The stirring continued for 0.5 h until the precipitation was complete, and then the mixture was filtered to obtain a crude product. The crude product was dissolved in 100 mL of NaOH solution with a mass fraction of 10% and acetic acid was added to adjust pH to 7. After suction filtration, the filter cake was washed with water and petroleum ether for several times to obtain intermediate 3.<sup>28</sup>

**2.2.4. General Synthetic Procedure for the Intermediate 4.** Water (100 mL) and ethanol (50 mL) were used as the reaction solvent, and 15 mol % *n*-bromosuccinimide was used as the catalyst. Salicylaldehyde (50 mmol) and 2,2-dimethyl-1,3-dioxane-4,6-dione acid (55 mmol) were reacted at room temperature for 10 h. After the end of the reaction, 50 mL of 20% ethanol was added to the reaction system and stirred at 100 °C for 10 min to remove impurities and catalysts. After sufficient cooling, suction filtration yields a pure intermediate 4.<sup>29</sup>

**2.2.5. General Synthetic Procedure for the Intermediate 5.** A mixture of coumarin-3-carboxylic acid (10.5 mmol) and DMF was added to a round-bottom flask containing a mixture of 1,2-dibromoethane (42 mmol) and triethylamine (21 mmol) for 6 h at room temperature. After the reaction was completed, the reaction mixture was poured into ice water and constantly stirred. When there was no solid precipitation, the obtained solid was dried at room temperature. And then the petroleum ether-ethyl acetate mixed solution (v/v = 3:1) was added for stirring overnight and filtered to obtain intermediate 5.<sup>30</sup>

**2.2.6. General Synthetic Procedure for Compounds A1–A38.** The intermediate 3 (6.43 mmol), K<sub>2</sub>CO<sub>3</sub> (12.86 mmol), and 30 mL of DMF were sequentially added to a 100 mL round-bottom flask. After stirring for 15 min at room temperature, intermediate 5 (6.43 mmol) was added. Reaction was monitored by TLC. Once the reaction was completed, the liquid was poured into ice water. It was then filtered to obtain a crude product. The crude product was purified by column chromatography to obtain the final target compounds A1–A38.<sup>30</sup>

**2.2.7. Antibacterial Activity Test In Vitro.** The antibacterial activity of 3-CCA derivatives against *Xoo*, *Rs*, and *Aac* was

assessed using the methodology outlined in a previously published research paper.<sup>31</sup> Bacterial strains were cultivated at a temperature of 37 °C in LB broth on a rotary shaker operating at 180 rpm until an optical density of 0.6 at 600 nm ( $OD_{600}$ ) was attained. Subsequently, 10  $\mu$ L of bacterial culture was combined with 190  $\mu$ L of LB broth to achieve concentrations of 50  $\mu$ g/mL. Kasugamycin and 3-CCA were used as the positive controls at the same concentration. As a control, equal volumes of DMSO were used as a vehicle control, with a maximum concentration of 1% DMSO. The 96-well plates were subjected to incubation at 28 °C, with shaking at 180 rpm for 12 h. The growth of bacteria was monitored by measuring the optical density at 600 nm, utilizing a microplate reader (Synergy H1, BioTek Instruments Inc., Vermont).

The virulences of potent antibacterial compounds against *Xoo* and *Aac* were tested at concentrations of 50, 25, 12.5, 6.25, and 3.125  $\mu$ g/mL, with three replicates per concentration. The determination of the 50% effective concentration ( $EC_{50}$ ) involved conducting a regression analysis on the percentage growth inhibition data, which was log-transformed to account for bactericide concentration.<sup>32</sup>

**2.2.8. Antibacterial Activities of A9 against *Aac* In Vivo.** The protective and curative effects of compound A9 against *Aac* were tested *in vivo* using a potting method. The test compound A9, dissolved in DMSO, was then diluted with 0.1% Tween-20 distilled water to get the concentrations of 200 and 100  $\mu$ g/mL. Seedlings of hybrid melon (cv. Yangjiaomi, obtained from China Vegetable Seed Technology Co., Ltd.) at the two true leaf stages were subjected to the potting test. To protect the leaves, the melon seedlings were subjected to spraying with either A9 or a control agent until complete saturation. Following a 24 h interval postspraying, the cotyledons were subsequently inoculated with *Aac* suspensions (with an  $OD_{600}$  of 1). The control seeds were treated with a solution of distilled water, DMSO, and Tween-20 in equal volumes. As positive controls, commercially available bactericides, namely 20% thiodiazole copper SC and 2% kasugamycin AS at a concentration of 100  $\mu$ g/mL, were employed. For the evaluation of the curative effect, compound A9 was sprayed to melon cotyledons 24 h after the aforementioned spraying procedure. The treated seedlings were then cultivated for 7 days under standard conditions, which included 16 h of light at a temperature of  $25 \pm 2$  °C and a relative humidity of  $60 \pm 5\%$ , followed by 8 h of darkness at a temperature of  $20 \pm 2$  °C and a relative humidity of  $75 \pm 5\%$ . Each treatment was measured on six plants, and each experimental condition was replicated 3 times.<sup>33</sup>

**2.2.9. Effect of A9 on the Growth of *Aac*.** The effect of A9 on the growth of *Aac* was assessed using a method outlined by Silva-Angulo et al.<sup>34</sup> with minor adjustments. *Aac* was cultivated in LB medium at 28 °C for 18 h with agitation at 180 rpm, followed by inoculation into LB medium supplemented with A9 to obtain final concentrations of 1/4 $EC_{50}$ , 1/2 $EC_{50}$ ,  $EC_{50}$ , 2 $EC_{50}$ , and 4 $EC_{50}$ . DMSO (1%) was used as a solvent control. Cultures were inoculated in 96-well plates and incubated at 28 °C with shaking at 180 rpm for 60 h. The optical density at 600 nm ( $OD_{600}$ ) was measured at 0, 1, 2, 4, 6, 8, 10, 12, and 24 h post-treatment. Each concentration was carried out in triplicate, and three independent experiments were performed.

**2.2.10. Effect of A9 on the Ultrastructure of *Aac*.** Scanning electron microscopy (SEM) was performed to evaluate the effect of compound A9 on the ultrastructure of *Aac*.<sup>35</sup> Bacterial

cultures ( $OD_{600} = 0.6$ ) were harvested by centrifugation at 5000 rpm for 5 min at 4 °C, followed by three washes with 0.1 mol/L phosphate buffer (PBS, pH 7.2). Bacterial suspensions were then treated with A9 dissolved in dimethyl sulfoxide (DMSO) to obtain the concentrations of 2 $EC_{50}$ . Control samples were prepared using solvent blanks of equal volume. The bacterial suspensions were incubated at 28 °C with shaking at 180 rpm for a duration of 24 h. The cells were harvested after centrifugation at 5000 rpm for 5 min at 4 °C. Subsequently, they were rinsed 3 times with a 0.1 mol/L PBS solution (pH 7.2). Following this, the samples were fixed for a period of 4 h in a 2.5% glutaraldehyde solution at a temperature of 4 °C. They were then washed 3 times for 5 min each in the same 0.1 mol/L PBS solution. The cells underwent dehydration using a sequential graded ethanol series (30, 50, 70, 80, 90, and 100%) for 15 min at each concentration, followed by a 20 min dehydration using 100% ethanol. After being freeze-dried for a duration of 8 h, the samples were coated with gold and examined for cell morphologies using a desktop scanning electron microscope (HITACHI SU8600).

**2.2.11. Effect of A9 on the Membrane Permeability of *Aac*.** The effect of A9 on the permeability of the cell membrane of *Aac* was examined using the method described by Ernst et al.<sup>36</sup> *Aac* cultures in the logarithmic growth phase (20 mL) were subjected to centrifugation at 2000 rpm for 5 min, followed by removal of the supernatant. Then, the cells were washed and resuspended in sterile water (20 mL). To get the concentrations of 1/2 $EC_{50}$ ,  $EC_{50}$ , 2 $EC_{50}$ , and 4 $EC_{50}$ , compound A9 dissolved in DMSO was diluted with the cell suspensions. The control measurements utilized DMSO as the solvent for the drugs, with a final concentration of 1%. Subsequently, the electric conductivity was measured and recorded at 0, 2, 4, 6, 8, and 12 h. To ensure accuracy and reliability, the experiment was repeated 3 times with triplicate samples for each concentration.

**2.2.12. Effect of A9 on Motility of *Aac*.** The effect of A9 on motility of *Aac* was previously described.<sup>37</sup> The *Aac* cultures were prepared by adjusting the initial  $OD_{600}$  to 0.6 and dissolving them in LB with 0.3% agar using microwave heating. A9 was then added at concentrations of  $EC_{50}$ , 2 $EC_{50}$ , and 4 $EC_{50}$ , with DMSO as the vehicle control. The media with A9 were poured into sterile Petri plates and allowed to solidify. A bacterial suspension (5  $\mu$ L) was inoculated onto the center of the semisolid medium and incubated at 28 °C for 48 h. Swimming motility was assessed by measuring the diameter of the covered areas.

**2.2.13. Effect of A9 on the Exopolysaccharide (EPS) Content of *Aac*.** The effect of A9 on the exopolysaccharide (EPS) content of *Aac* was performed according to the means of Shi et al.<sup>38</sup> The DMSO solutions containing A9 were diluted with bacterial suspensions ( $OD_{600} = 0.6$ ) to achieve the final concentrations of  $EC_{50}$ , 2 $EC_{50}$ , and 4 $EC_{50}$ , and subsequently incubated at 28 °C with continuous shaking at 180 rpm for 72 h. An equivalent concentration of the solvent (DMSO) was used as a control. The supernatant was collected following centrifugation at 3000 rpm for 20 min at 4 °C. The exopolysaccharides (EPS) were precipitated using three volumes of absolute ethanol and allowed to settle overnight. After subsequent centrifugation, the samples were oven-dried at 70 °C to a constant weight for weighing. This process was repeated 3 times with each assay being performed in triplicate.

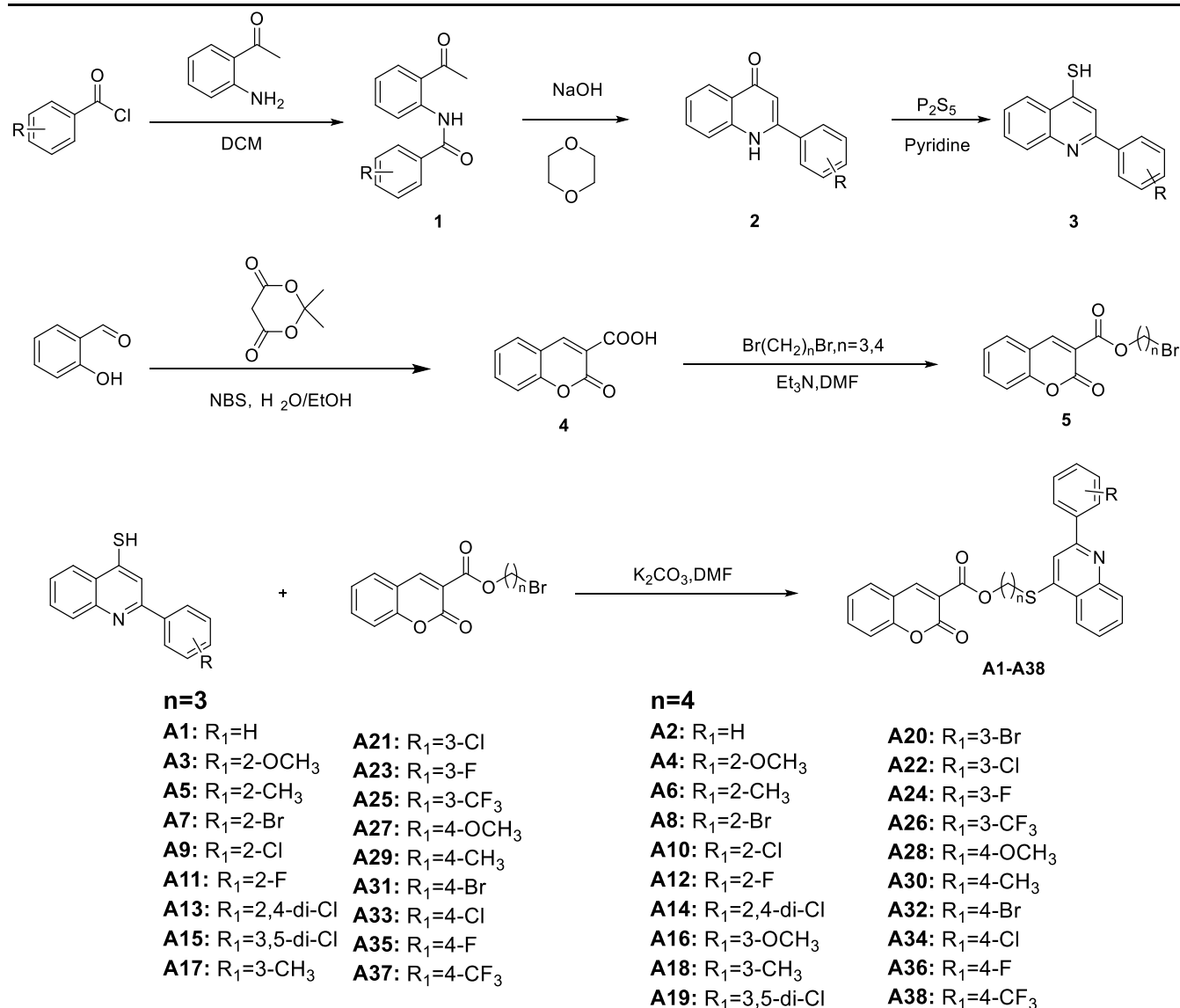


**Figure 1.** Synthesis route of the target compounds.

**2.2.14. Effect of A9 on the Biofilm Formation of Aac.** The effect of **A9** on the biofilm formation of *Aac* was assessed according to the method previously described by Du et al.<sup>39</sup> with slight alteration. The bacterium was cultured in LB broth at 28 °C with shaking at 180 rpm for 18 h, followed by centrifugation and adjustment to an OD<sub>600</sub> of 1. Gradient dilutions of **A9** (EC<sub>50</sub>, 2EC<sub>50</sub>, and EC<sub>50</sub>) were introduced into sterile borosilicate glass tubes. Negative controls were established by adding bacterial cultures and an agent dilution buffer (100 μL of each). The test tubes were subsequently incubated at 28 °C for 2 days. Biofilms of *Aac* were stained with 0.1% crystal violet solution for 1 h and then washed 3 times with deionized water to remove excess crystal violet stain. The biofilms were diluted with 10% glacial acetic acid for a duration of 1 h. Optical density at 600 nm (OD<sub>600</sub>) was measured following the transfer of 200 μL of the culture into a 96-well plate. Each concentration treatment was conducted in sextuplicate, and the entire experimental procedure was replicated 3 times.

**2.2.15. Statistical Analysis.** The results were expressed as means ± standard error (SE) based on three independent

repeated experiments. A variance analysis was conducted using SPSS software (version 20.0, IBM Corp., Armonk, NY) to analyze the data. To determine statistical significance, Duncan's multiple range test was employed at a significance level of  $P < 0.05$ . Graphs were created using Sigma Plot (version 12.5, Systat Software Inc., San Jose, CA).

### 3. RESULTS AND DISCUSSION

**3.1. Chemistry.** The synthetic route for the synthesis of coumarin-3-carboxylic acid derivatives containing a thioether quinoline moiety is depicted in Figure 1. The structures of these derivatives were characterized using <sup>1</sup>H NMR, <sup>13</sup>C NMR, and HRMS techniques. Initially, 2-aminophenone was subjected to reaction with various substituted benzoyl chlorides to yield intermediate **1**. Subsequently, intramolecular condensation of intermediate **1** was carried out employing Combes quinoline synthesis, resulting in the formation of intermediate **2**. Furthermore, the utilization of phosphorus pentasulfide in the subsequent step led to the formation of intermediate **3**.

synthesized through cyclization utilizing salicylaldehyde as the starting material, and **intermediate 4** underwent a reaction with dibromoalkane to obtain **intermediate 5**. Ultimately, a substitution reaction between **intermediate 3** and **intermediate 5** achieved compounds **A1**–**A38**.

**3.2. Antibacterial Activity of 3-CCA Derivatives against *Xoo*, *Rs*, and *Aac* In Vitro.** The *in vitro* antibacterial activities of thirty-eight derivatives containing a thioether quinoline moiety were assessed against *Xoo*, *Rs* and *Aac*, as indicated in **Table 1**. The results revealed that these compounds exhibited greater efficacy against *Xoo* and *Aac*, while displaying lower antibacterial activity against *Rs*. Notably, compound **A9** and **A13** demonstrated the highest antibacterial potential against *Xoo* and *Aac*, with inhibition rates of 90.68, 89.29 and 93.71, 84.10% at 50  $\mu\text{g/mL}$ , respectively. These rates were superior to those of 3-CCA and comparable to the

**Table 1. Antibacterial Activity of 38 Compounds against *Xoo*, *Rs*, and *Aac***

compound	<i>n</i>	R	inhibition rate (%)		
			<i>Xoo</i>	<i>Rs</i>	<i>Aac</i>
A1	3	H	76.05	35.57	60.21
A2	4	H	78.18	34.43	54.78
A3	3	2-OCH <sub>3</sub>	18.89	39.60	17.51
A4	4	2-OCH <sub>3</sub>	1.36	40.87	14.62
A5	3	2-CH <sub>3</sub>	9.50	8.10	25.38
A6	4	2-CH <sub>3</sub>	22.38	18.60	19.05
A7	3	2-Br	44.2	30.93	67.22
A8	4	2-Br	39.03	22.6	54.1
A9	3	2-Cl	90.68	44.62	93.71
A10	4	2-Cl	76.64	35.8	71.32
A11	3	2-F	64.76	26.66	63.35
A12	4	2-F	58.12	40.05	61.14
A13	3	2,4-di-Cl	89.29	27.31	84.1
A14	4	2,4-di-Cl	65.47	18.89	2.72
A15	3	3,5-di-Cl	25.49	7.60	17.90
A16	4	3-OCH <sub>3</sub>	30.75	40.3	69.37
A17	3	3-CH <sub>3</sub>	42.62	37.28	67.26
A18	4	3-CH <sub>3</sub>	38.26	36.05	46.91
A19	4	3,5-di-Cl	32.92	22.96	22.25
A20	4	3-Br	18.43	20.29	3.29
A21	3	3-Cl	47.88	33.72	20.25
A22	4	3-Cl	35.75	23.14	2.05
A23	3	3-F	73.30	15.00	18.99
A24	4	3-F	25.10	13.28	26.94
A25	3	3-CF <sub>3</sub>	79.13	16.60	20.89
A26	4	3-CF <sub>3</sub>	51.04	10.37	8.37
A27	3	4-OCH <sub>3</sub>	72.87	42.29	47.65
A28	4	4-OCH <sub>3</sub>	64.23	21.65	4.72
A29	3	4-CH <sub>3</sub>	66.37	40.02	69.58
A30	4	4-CH <sub>3</sub>	71.24	42.51	65.87
A31	3	4-Br	55.69	22.70	14.11
A32	4	4-Br	45.80	27.12	11.30
A33	3	4-Cl	72.51	24.52	53.86
A34	4	4-Cl	70.83	26.35	61.56
A35	3	4-F	82.76	34.76	72.87
A36	4	4-F	69.08	34.85	63.93
A37	3	4-CF <sub>3</sub>	71.43	21.75	33.12
A38	4	4-CF <sub>3</sub>	79.04	34.31	57.46
3-CCA			64.92	51.24	56.44
kasugamycin			90.14	78.3	95.24

positive control kasugamycin, which suggested promising antibacterial properties. Compound **A35** exhibited superior antibacterial activity against *Xoo* and *Aac* in comparison to 3-CCA, albeit inferior to the positive control kasugamycin. Conversely, compound **A25** demonstrated selectivity against *Xoo*, displaying enhanced antibacterial efficacy against *Xoo* relative to 3-CCA, yet still falling short of the positive control kasugamycin.

**3.3. Structure–Activity Relationship Analysis.** The antibacterial activity test data revealed that the biological activity of the compounds was greatly influenced by the length of the carbon chain and the type of substituent. Specifically, compounds with a carbon chain length of three exhibit significantly enhanced antibacterial activity compared to that of other compounds. For instance, compounds **A9** (*n* = 3), **A13** (*n* = 3), and **A35** (*n* = 3) demonstrate this effect. Furthermore, the introduction of a single substituent, particularly an electron-withdrawing group, at position 2 of the benzene ring also affects the antibacterial activity. The bactericidal activity of compound **A9** (R = 2-Cl) exhibits significant improvement. However, the introduction of single substituents at positions 3 and 4 did not contribute to the enhancement of activity. The relationship between structure and activity is intricate, and the impact of introduced substituents on activity was contingent on the bacterial category. In the case of *Xoo*, the inclusion of electron-withdrawing groups resulted in higher bactericidal activity, exemplified by compounds **A25** (R = 3-CF<sub>3</sub>) and **A35** (R = 4-F). The bactericidal activity of *Rs* was enhanced by the introduction of electron contributing groups, as observed in compounds **A16** (R = 3-OCH<sub>3</sub>) and **A30** (R = 4-CH<sub>3</sub>). Similarly, the bactericidal activity of *Aac* is increased when electron contributing groups were introduced, as demonstrated by compounds **A17** (R = 3-CH<sub>3</sub>) and **A29** (R = 4-CH<sub>3</sub>). Notably, the introduction of a double substituent on the terminal benzene ring, particularly at positions 2 and 4, significantly contributed to the observed activity enhancement, exemplified by compound **A13** (R = 2,4-di-Cl).

**3.4. Bacterial Virulence Assays of High-Activity Compounds.** Based on the findings from **Section 3.2**, an assessment was conducted to evaluate the virulence of the high-activity compounds against *Xoo* and *Aac*, as indicated in **Table 2**. The outcomes revealed that **A9** exhibited the most robust antibacterial activity against *Xoo* and *Aac*, as evidenced by the EC<sub>50</sub> values of 11.05 and 8.05  $\mu\text{g/mL}$ , respectively. This performance surpassed that of 3-CCA and was comparable to the antibacterial effect observed with positive control kasugamycin. Additionally, compound **A35** demonstrated marked bactericidal activity against *Xoo* and *Aac*, with EC<sub>50</sub> values of 14.87 and 15.42  $\mu\text{g/mL}$ , respectively, which were equivalent to the antibacterial potency of **A9**. The remaining compounds had moderate antibacterial activity against *Xoo* and *Aac*, with EC<sub>50</sub> values ranging from 11 to 32  $\mu\text{g/mL}$ .

**3.5. Bacterial Activity of A9 against *Aac* In Vivo.** According to the findings presented in **Table 3** and **Figure 2**, it is evident that **A9** exhibits robust protective and curative effects against *Aac* *in vivo*. The efficacy rates for **A9** are recorded at 61.50 and 54.86%, respectively, which are notably lower than the positive control kasugamycin (67.57, 60.71%), but superior to the positive control thiodiazole copper (51.89, 48.94%).

**3.6. Growth Curve.** The effect of varying concentrations of **A9** on the growth curves of *Aac* was investigated, with the results depicted in **Figure 3**. Treatment with **A9** exhibited a

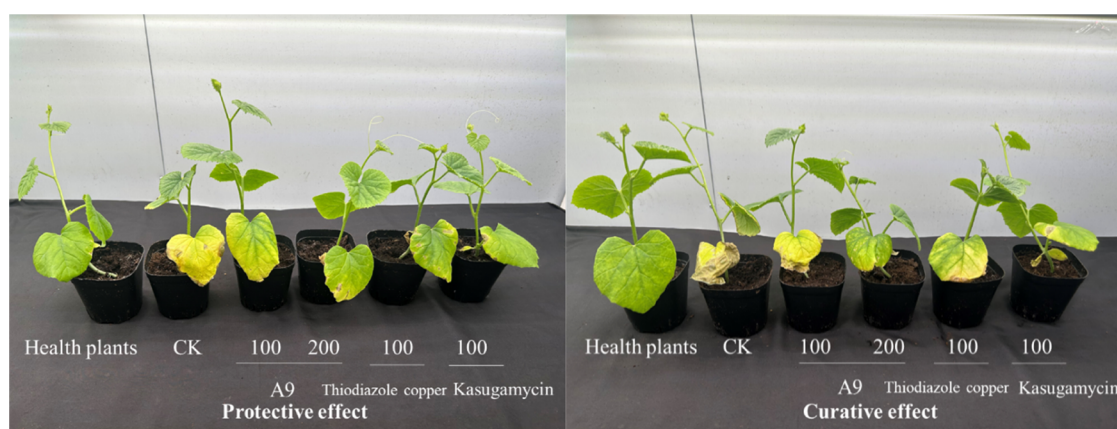
Table 2. Antibacterial Virulence of the High-Activity Compounds against *Xoo* and *Aac*

bacteria	compound	LC-P	r	EC <sub>50</sub> (μg/mL)	95%FL (μg/mL)
<i>Xoo</i>	A1	2.85 + 1.71x	0.96	18.12	12.68–25.89
	A7	2.58 + 1.98x	0.95	16.7	11.98–23.30
	A9	3.42 + 1.52x	0.97	11.05	7.03–17.36
	A10	2.06 + 2.79x	0.96	11.26	9.13–13.88
	A11	2.58 + 2.03x	0.99	15.55	11.20–21.58
	A12	2.48 + 1.72x	0.98	29.09	20.84–40.59
	A13	3.59 + 1.17x	0.99	16.34	10.73–24.87
	A23	1.90 + 2.36x	0.98	20.72	15.84–27.09
	A27	2.26 + 2.03x	0.97	22.42	16.65–30.19
	A29	2.62 + 1.65x	0.97	27.91	19.69–39.55
	A35	3.29 + 1.46	0.99	14.87	10.51–21.05
	A38	2.73 + 1.76x	0.99	19.42	13.81–27.30
	3-CCA	2.58 + 1.63x	0.97	30.37	21.27–43.37
	kasugamycin	3.76 + 1.16x	0.99	11.65	6.95–19.53
<i>Aac</i>	A1	1.45 + 2.34x	0.97	32.65	25.15–42.38
	A9	3.42 + 1.74x	0.99	8.05	5.75–11.27
	A11	2.99 + 1.38x	0.99	28.15	18.86–42.01
	A13	2.87 + 1.52x	0.98	24.95	17.59–35.40
	A17	3.12 + 1.43x	0.98	20.71	13.88–30.89
	A35	2.79 + 1.86x	0.99	15.42	11.63–20.45
	3-CCA	3.23 + 1.1x	0.98	39.48	24.51–63.58
	kasugamycin	3.45 + 1.37x	0.97	13.55	8.81–20.83

Table 3. Protective and Curative Effects of A9 against *Aac* In Vivo<sup>a</sup>

sample	concentration (μg/mL)	protective effect		curative effect	
		disease index	efficacy (%)	disease index	efficacy (%)
A9	200	10.56 ± 1.11c	61.5b	15.56 ± 0.96d	54.86b
	100	15.37 ± 0.85b	43.9d	22.96 ± 0.64b	33.32d
thiodiazole copper	100	13.15 ± 0.32c	51.89c	17.59 ± 0.85c	48.94c
kasugamycin	100	8.89 ± 0.56d	67.57a	13.52 ± 0.32e	60.71a
CK		27.41 ± 1.70a		34.44 ± 1.11a	

<sup>a</sup>Columns represent the mean ± SE. Different letters in the column represent significant difference at the  $P_{0.05}$  level, the same as following.

Figure 2. Protective and curative effects of A9 against *Aac* in vivo.

significant inhibitory effect on *Aac* growth, showing a concentration-dependent relationship across concentrations ranging from 1/4 to 4EC<sub>50</sub>.

**3.7. Bacterial Morphology.** The effect of A9 on the ultramicrostructure of *Aac* is illustrated in Figure 4. The surface morphology of the control cells exhibited a rounded and full appearance, while the cells treated with A9 displayed an irregular shape with sunken and wrinkled surfaces.

**3.8. Cell Membrane Permeability.** The results showed a positive correlation between A9 concentrations and electric conductivity, with a notable increase observed in relative electric conductivity within the first 4 h of treatment in Figure 5. Subsequently, the rate of increase slowed down, leading to a final relative conductivity of 81.13% at 4EC<sub>50</sub> after 12 h of treatment, surpassing both the control and other treatments.

**3.9. Swimming Assay.** As showcased in Figure 6, the presence of A9 had a significant impact on the motility of *Aac*.

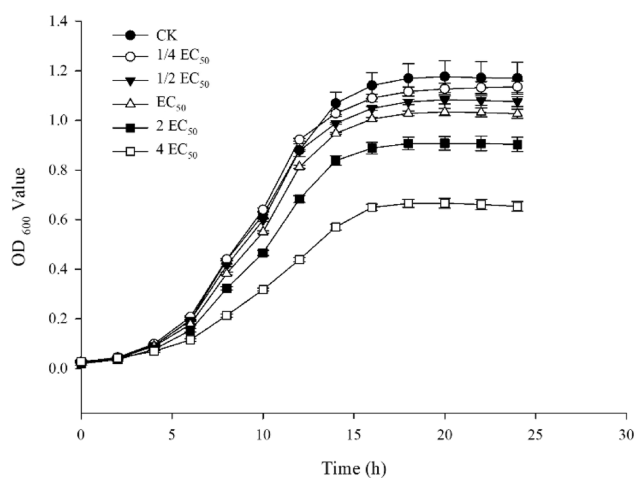


**Figure 3.** Effect of A9 concentration on the growth of *Aac*.

The swimming diameter of A9 against *Aac* measured 1.04 mm at  $4EC_{50}$ , indicating a statistically superior performance compared with both the control group and other treatments.

**3.10. EPS Content.** As demonstrated in Figure 7, A9 exhibits a significant impact on the production of exopolysaccharides from *Aac*. The production of exopolysaccharides from *Aac* decreased to 11.03, 10.65, and 9.60 mg at the concentrations of  $EC_{50}$ ,  $2EC_{50}$ , and  $4EC_{50}$ , resulting in reductions of 12.66, 15.70, and 24.01%, respectively, compared to the control.

**3.11. Biofilm Formation Assay.** As shown in Figure 8, A9 exhibits inhibitory effects on the biofilm formation of *Aac*. These inhibitory effects were found to be positively associated with the concentrations at which the treatment was administered. Specifically, the biofilm formation of *Aac* reduced to 19.56, 26.69, and 36.15% at  $EC_{50}$ ,  $2EC_{50}$ , and  $4EC_{50}$ , respectively.

#### 4. CONCLUSIONS

In summary, this study employed the active splicing principle to synthesize a range of coumarin-3-carboxylic acid derivatives featuring a thioether quinoline moiety. Subsequently, the biological activity of these derivatives was assessed. The results of the antibacterial assay indicated that the majority of the compounds displayed significant antibacterial activity against *Xoo*, *Rs*, and *Aac*. Particularly, compound A9 exhibited the

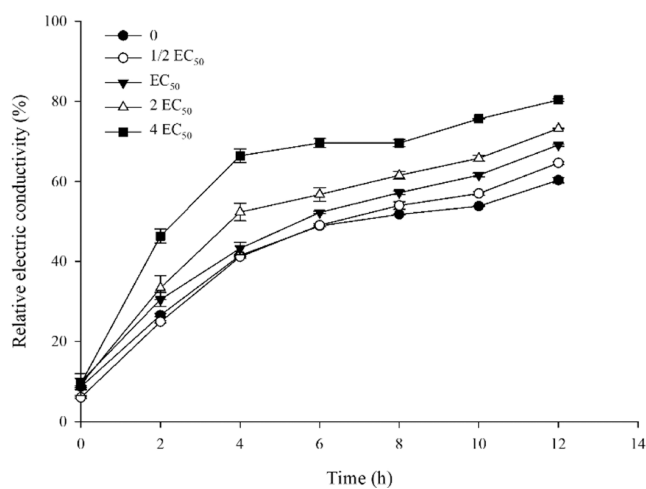


**Figure 5.** Effect of compound A9 on cell membrane permeability of *Aac*.

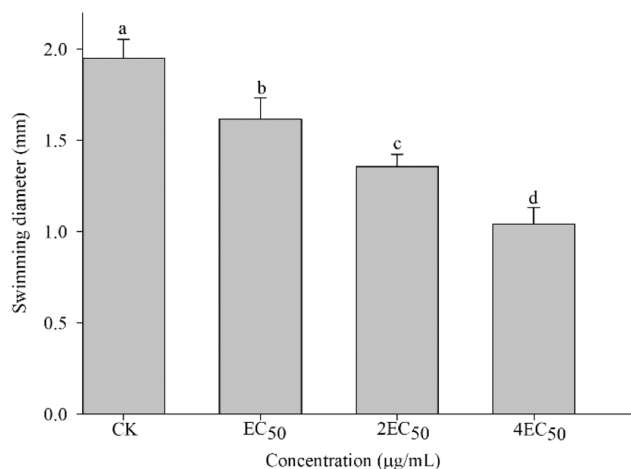


**Figure 6.** Effect of A9 on bacterial motility of *Aac*.

most potent activity against *Aac* both *in vitro* and *in vivo*. Further toxicological investigations revealed that the inhibition of bacterial growth in *Aac* was attributed to induce alterations in cell morphology, damage to the bacterial cell membrane, decrease motility, reduce exopolysaccharide production, and prevention of biofilm formation. Consequently, these innova-

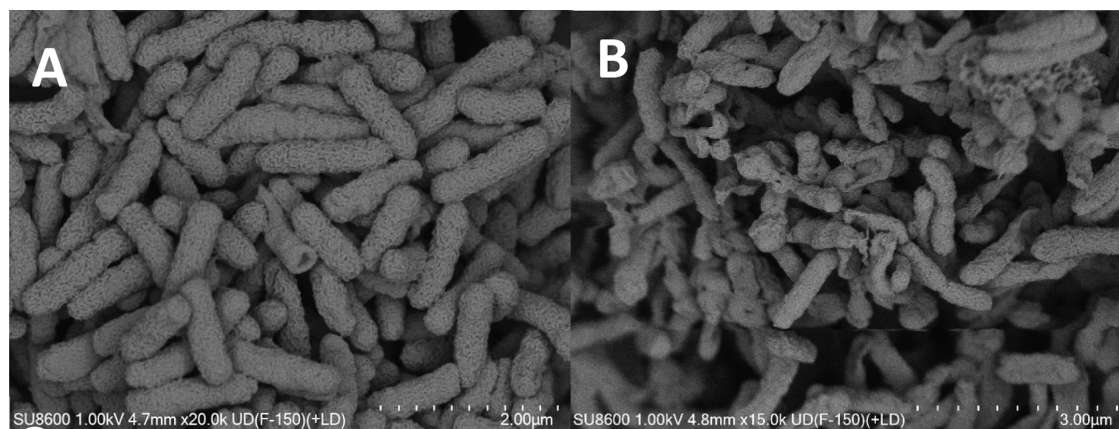


**Figure 4.** SEM observations of conAac treated with A9.

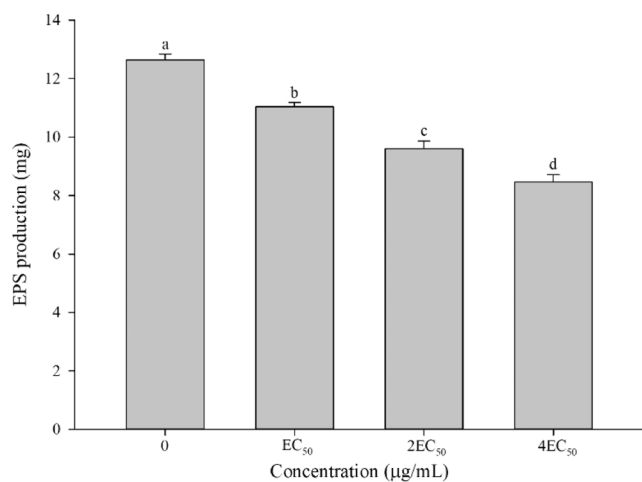


Figure 7. Effect of A9 on the EPS content of Aac.

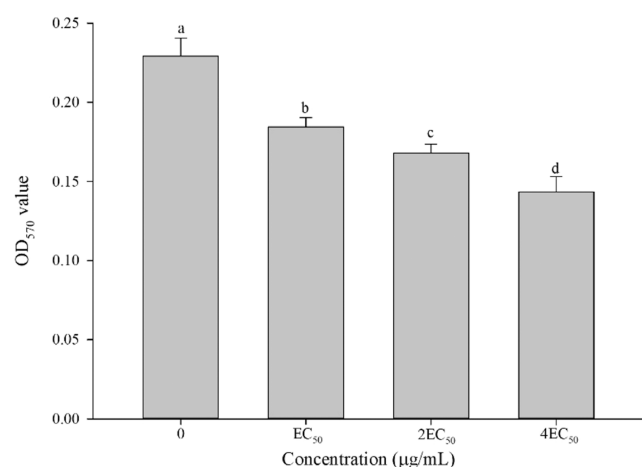


Figure 8. Effect of A9 on the biofilm formation of Aac.

tive derivatives of coumarin-3-carboxylic acid, incorporating a thioether quinoline moiety, hold promise as potential alternative frameworks for the development of novel antibacterial agents.

## ■ ASSOCIATED CONTENT

### SI Supporting Information

The Supporting Information is available free of charge at <https://pubs.acs.org/doi/10.1021/acsomega.4c08627>.

Characterizations data; <sup>1</sup>H, <sup>13</sup>C, and <sup>19</sup>F NMR spectra and HRMS of title compounds are provided (PDF)

## ■ AUTHOR INFORMATION

### Corresponding Authors

**Jing Zhang** – Environment and Plant Protection Institute, Chinese Academy of Tropical Agricultural Science, Haikou 571101, China; Phone: 0086-898-66969260; Email: [zh-jing99@163.com](mailto:zh-jing99@163.com); Fax: 0086-898-66969211

**Gang Feng** – Environment and Plant Protection Institute, Chinese Academy of Tropical Agricultural Science, Haikou 571101, China; [orcid.org/0009-0007-0723-6488](https://orcid.org/0009-0007-0723-6488); Phone: 0086-898-66969260; Email: [feng8513@sina.com](mailto:feng8513@sina.com); Fax: 0086-898-66969211

## Authors

**Yuanquan Zhang** – National Key Laboratory of Green Pesticide, Key Laboratory of Green Pesticide and Agricultural Bioengineering, Ministry of Education, Center for R&D of Fine Chemicals of Guizhou University, Guiyang 550025, China; Environment and Plant Protection Institute, Chinese Academy of Tropical Agricultural Science, Haikou 571101, China

**Zhiyuan Xu** – Environment and Plant Protection Institute, Chinese Academy of Tropical Agricultural Science, Haikou 571101, China

**Minxiang Dou** – Environment and Plant Protection Institute, Chinese Academy of Tropical Agricultural Science, Haikou 571101, China

**Yan Xu** – Environment and Plant Protection Institute, Chinese Academy of Tropical Agricultural Science, Haikou 571101, China

**Xin Fu** – Environment and Plant Protection Institute, Chinese Academy of Tropical Agricultural Science, Haikou 571101, China

**Fadi Zhu** – Environment and Plant Protection Institute, Chinese Academy of Tropical Agricultural Science, Haikou 571101, China

**Huochun Ye** – Environment and Plant Protection Institute, Chinese Academy of Tropical Agricultural Science, Haikou 571101, China

Complete contact information is available at:

<https://pubs.acs.org/10.1021/acsomega.4c08627>

## Author Contributions

<sup>§</sup>Yuanquan Zhang, Zhiyuan Xu, and Minxiang Dou contributed equally to this work.

## Notes

The authors declare no competing financial interest.

## ■ ACKNOWLEDGMENTS

This work was supported financially by the Key Research Development Program of Hainan Province, China (ZDYF2024XDNY202), the Natural Science Foundation of China (32372598), Chinese Academy of Tropical Agricultural Sciences for Science and Technology Innovation Team of National Tropical Agricultural Science Center (CAT-ASCXTD202410), Central Public-interest Scientific Institution Basal Research Fund (1630042024020).

## ■ ABBREVIATIONS

<sup>1</sup>H NMR; <sup>1</sup>H nuclear magnetic resonance; <sup>13</sup>C NMR; <sup>13</sup>C nuclear magnetic resonance; HRMS; high-resolution mass spectrometry; EC<sub>50</sub>; median effective concentration; 3-CCA; coumarin-3-carboxylic acid; SEM; scanning electron microscopy; DMSO; Dimethylsulfoxide; *Xoo*; *Xanthomonas oryzae* pv. *oryzae*; *Rs*; *Ralstonia solanacearum*; *Aac*; *Acidovorax citrulli*

## ■ REFERENCES

- Huang, X.; Liu, H. W.; Long, Z. Q.; Li, Z. X.; Zhu, J. J.; Wang, P. Y.; Qi, P. Y.; Liu, L. W.; Yang, S. Rational Optimization of 1,2,3-Triazole-Tailored Carbazoles As Prospective Antibacterial Alternatives with Significant In Vivo Control Efficiency and Unique Mode of Action. *J. Agric. Food Chem.* **2021**, *69* (16), 4615–4627.
- Ogunyemi, S. O.; Abdullah, Y.; Ibrahim, E.; Zhang, Y.; Bi, J.; Wang, F.; Ahmed, T.; Alkhalifah, D. H. M.; Hozzein, W. N.; Yan, C. Q.; Li, B.; Xu, L. H. Bacteriophage-mediated biosynthesis of



MnO<sub>2</sub>NPs and MgONPs and their role in the protection of plants from bacterial pathogens. *Front. Microbiol.* **2023**, *14*, No. 1193206.

(3) Li, P.; Hu, D. Y.; Xie, D. D.; Chen, J. X.; Jin, L. H.; Song, B. A. Design, Synthesis, and Evaluation of New Sulfone Derivatives Containing a 1,3,4-Oxadiazole Moiety as Active Antibacterial Agents. *J. Agric. Food Chem.* **2018**, *66* (12), 3093–3100.

(4) Kumar, R.; Barman, A.; Phukan, T.; Kabyashree, K.; Ray, S. K.; et al. *Ralstonia solanacearum* virulence in tomato seedlings inoculated by leaf clipping. *Plant Pathol.* **2017**, *66* (66), 835–841.

(5) Rahimi-Midani, A.; Kim, J. O.; Kim, J. H.; Lim, J.; Ryu, J. G.; Kim, M. K.; Choi, T. J. Potential use of newly isolated bacteriophage as a biocontrol against *Acidovorax citrulli*. *Arch. Microbiol.* **2020**, *202* (2), 377–389.

(6) Orfei, B.; Moretti, C.; Loreti, S.; Tatulli, G.; Onofri, A.; Scotti, L.; Aceto, A.; Buonauro, R. Silver nanoclusters with Ag<sub>2</sub>+3+ oxidative states are a new highly effective tool against phytopathogenic bacteria. *Appl. Microbiol. Biotechnol.* **2023**, *107* (14), 4519–4531.

(7) Yang, T.; Zhang, T.; Zhou, X.; Wang, P. Y.; Gan, J. H.; Song, B. A.; Yang, S.; Yang, C. G. Dysregulation of ClpP by Small-Molecule Activators Used Against *Xanthomonas oryzae* pv. *oryzae* Infections. *J. Agric. Food Chem.* **2021**, *69* (27), 7545–7553.

(8) Zhang, Z.; Bai, Z.; Ling, Y.; He, L.; Huang, P.; Gu, H.; Hu, R. F. Design, synthesis and biological evaluation of novel furoxan-based coumarin derivatives as antitumor agents. *Med. Chem. Res.* **2018**, *27* (4), 1198–1205.

(9) Chimenti, F.; Secci, D.; Bolasco, A.; Chimenti, P.; Granese, A.; Befani, O.; et al. Inhibition of monoamine oxidases by coumarin-3-acyl derivatives: biological activity and computational study. *Bioorg. Med. Chem. Lett.* **2004**, *14* (14), 3697–3703.

(10) Ji, H.; Tan, Y.; Gan, N.; Zhang, J.; Li, S.; Zheng, X.; et al. Synthesis and anticancer activity of new coumarin-3-carboxylic acid derivatives as potential lactate transport inhibitors. *Bioorg. Med. Chem.* **2021**, *29*, No. 115870.

(11) Wei, L.; Wang, J.; Zhang, X.; Wang, P.; Zhao, Y.; Li, J.; et al. Discovery of 2H-chromen-2-one derivatives as G protein-coupled receptor-35 agonists. *J. Med. Chem.* **2017**, *60* (1), 362–372.

(12) Lin, P. Y.; Yeh, K. S.; Su, C. L.; Sheu, S. Y.; Chen, T.; Ou, K. L.; et al. Synthesis and antibacterial activities of novel 4-hydroxy-7-hydroxy- and 3-carboxycoumarin derivatives. *Molecules* **2012**, *17* (9), 10846–10863.

(13) Liu, H.; Ren, Z. L.; Wang, W.; Gong, J. X.; Chu, M. J.; Ma, Q. W.; et al. Novel coumarin-pyrazole carboxamide derivatives as potential topoisomerase II inhibitors: design, synthesis and antibacterial activity. *Eur. J. Med. Chem.* **2018**, *157*, 81–87.

(14) Zhu, F. D.; Fu, X.; Ye, H. C.; Ding, H. X.; Gu, L. S.; Zhang, J.; Guo, Y. X.; Feng, G. Antibacterial activities of coumarin-3-carboxylic acid against *Acidovorax citrulli*. *Front. Microbiol.* **2023**, *14* (14), No. 1207125.

(15) Yu, X.; Teng, P.; Zhang, Y. L.; Xu, Z. J.; Zhang, M. Z.; Zhang, W. H. Design, synthesis and antifungal activity evaluation of coumarin-3-carboxamide derivatives. *Fitoterapia* **2018**, *127*, 387–395.

(16) Liang, J. C.; Fu, X.; Zhang, J.; Ding, H. X.; Xu, Z. Y.; Ye, H. C.; Zhu, F. D.; Yan, C.; Gan, X. H.; Feng, G. Design, synthesis and antibacterial activity of coumarin-3-carboxylic acid derivatives containing acylhydrazone moiety. *Arabian J. Chem.* **2024**, *17*, No. 105389.

(17) Wei, L.; Wang, J.; Zhang, X.; Wang, P.; Zhao, Y.; Li, J.; et al. Discovery of 2H-chromen-2-one derivatives as G protein-coupled receptor-35 agonists. *J. Med. Chem.* **2017**, *60*, 362–372.

(18) El Shehry, M. F.; Ghorab, M. M.; Abbas, S. Y.; Fayed, E. A.; Shedid, S. A.; Ammar, Y. A. Quinoline derivatives bearing pyrazole moiety: Synthesis and biological evaluation as possible antibacterial and antifungal agents. *Eur. J. Med. Chem.* **2018**, *143*, 1463–1473.

(19) Zhang, M. Z.; Jia, C. Y.; Gu, Y. C.; Mulholland, N.; Turner, S.; Beattie, D.; Zhang, W. H.; Yang, G. F.; Clough, J. Synthesis and antifungal activity of novel indole-replaced streptochlorin analogues. *Eur. J. Med. Chem.* **2017**, *126*, 669–674.

(20) Jones, R. A.; Panda, S. S.; Hall, C. D. Quinine conjugates and quinone analogues as potential antimalarial agents. *Eur. J. Med. Chem.* **2015**, *97*, 335–355.

(21) Tseng, C. H.; Tzeng, C. C.; Yang, C. L.; Lu, P. J.; Chen, H. L.; Li, H. Y.; Chuang, Y. C.; Yang, C. N.; Chen, Y. L. Synthesis and antiproliferative evaluation of certain indeno[1,2-c]quinoline derivatives. Part 2. *J. Med. Chem.* **2010**, *53*, 6164–6179.

(22) Liu, F.; Zhang, X.; Weisberg, E.; Chen, S.; Hur, W.; Wu, H.; Zhao, Z.; Wang, W.; Mao, M.; Cai, C.; Simon, N. I.; Sanda, T.; Wang, J.; Look, A. T.; Griffin, J. D.; Balk, S. P.; Liu, Q.; Gray, N. S. Discovery of a selective irreversible BMX inhibitor for prostate cancer. *ACS Chem. Biol.* **2013**, *8*, 1423–1428.

(23) Adsule, S.; Barve, V.; Chen, D.; Ahmed, F.; Dou, Q. P.; Padhye, S.; Sarkar, F. H. Novel schiff base copper complexes of quinoline-2-carboxaldehyde as proteasome inhibitors in human prostate cancer cells. *J. Med. Chem.* **2006**, *49*, 7242–7246.

(24) Karad, S. C.; Purohit, V. B.; Thakor, P.; Thakkar, V. R.; Raval, D. K. Novel morpholinoquinoline nucleus clubbed with pyrazoline scaffolds: Synthesis, antibacterial, antitubercular and antimalarial activities. *Eur. J. Med. Chem.* **2016**, *112*, 270–279.

(25) Thomas, K. D.; Adhikari, A. V.; Telkar, S.; Chowdhury, I. H.; Mahmood, R.; Pal, N. K.; Row, G.; Sumesh, E. Design, synthesis and docking studies of new quinoline-3-carbohydrazide derivatives as antitubercular agents. *Eur. J. Med. Chem.* **2011**, *46*, 5283–5292.

(26) Chioua, M.; Sucunza, D.; Soriano, E.; Hadjipavlou-Litina, D.; Alcazar, A.; Ayuso, I.; Oset-Gasque, M. J.; Gonzalez, M. P.; Monjas, L.; Rodriguez-Franco, M. I.; Marco-Contelles, J.; Samadi, A. Alphaaryl-N-alkyl nitrones, as potential agents for stroke treatment: synthesis, theoretical calculations, antioxidant, anti-inflammatory, neuroprotective, and brain-blood barrier permeability properties. *J. Med. Chem.* **2012**, *55*, 153–168.

(27) Wang, Q. F.; Xing, L.; Zhang, Y. Q.; Gong, C. Y.; Zhou, Y. X.; Zhang, N.; He, B. C.; Xue, W. Antiviral activity evaluation and action mechanism of myricetin derivatives containing thioether quinoline moiety. *Mol. Diversity* **2023**, *3*, 1039–1055.

(28) Yang, R.; Ma, Y. N.; Huang, T.; Xie, W.; Zhang, X.; Huang, G. S.; Liu, X. D. Synthesis and Antifungal Activities of 4-Thioquinoline Compounds. *Chin. J. Org. Chem.* **2018**, *38* (8), 2143–2150.

(29) Ruan, H. L.; Zhang, J. Y.; Sun, S.; Wang, Y.; Zhu, X. L.; Lü, C. W. N-Bromosuccinimide Mediated the Reaction of 2-Hydroxyaryl Aldehydes with Meldrum's Acid for Synthesis of Coumarin-3-carboxylic Acids. *Chin. J. Org. Chem.* **2017**, *37* (8), 2139–2144.

(30) Peng, F.; Liu, T. T.; Cao, X.; Wang, Q. F.; Liu, F.; Liu, L. W.; He, M.; Xue, W. Antiviral activities of novel myricetin derivatives containing 1,3,4-oxadiazole bithioether. *Chem. Biodiversity* **2022**, *19* (3), No. e202100939.

(31) Zhiyuan, X.; Haixin, D.; Xin, F.; Yan, X.; Fadi, Z.; Huochun, Y.; Yuan, Z. Y.; Yongxia, G.; Jing, Z.; Gang, F. Antibacterial activity and possible mechanism of action of isoquinoline-3-carboxylic acid. *Nat. Prod. Commun.* **2024**, DOI: 10.1177/1934578x241226562.

(32) Li, G. H.; Qiao, M. Y.; Guo, Y.; Wang, X.; Xu, Y. F.; Xia, X. D. Effect of subinhibitory concentrations of chlorogenic acid on reducing the virulence factor production by *Staphylococcus aureus*. *Foodborne Pathog. Dis.* **2014**, *11*, 677–683.

(33) Li, B.; Shi, Y.; Shan, C. L.; Zhou, Q.; Ibrahim, M.; Wang, Y. L.; Wu, G. X.; Li, H. Y.; Xie, G. L.; Sun, G. C. Effect of chitosan solution on the inhibition of *Acidovorax citrulli* causing bacterial fruit blotch of watermelon. *J. Sci. Food Agric.* **2013**, *93*, 1010–1015.

(34) Silva-Angulo, A. B.; Zanini, S. F.; Rosenthal, A.; Rodrigo, D.; Klein, G.; Martínez, A. Comparative study of the effects of citral on the growth and injury of *Listeria innocua* and *Listeria monocytogenes* cells. *PLoS One.* **2015**, *10*, No. e0114026.

(35) Wang, T. L.; Guan, W.; Huang, Q.; Yang, Y. W.; Yan, W. R.; Sun, B. X.; Zhao, T. C. Quorum-sensing contributes to virulence, twitching motility, seed attachment and biofilm formation in the wild type strain Aac-5 of *Acidovorax citrulli*. *Microb. Pathog.* **2016**, *100*, 133–140.

(36) Ernst, W. A.; Thoma-Uszynski, S.; Teitelbaum, R.; Ko, C.; Hanson, D. A.; Clayberger, C.; Krensky, A. M.; Leippe, M.; Bloom, B.

R.; Ganz, T.; Modlin, R. L. Granulysin, a T cell product, kills bacteria by altering membrane permeability. *J. Immunol.* **2000**, *165*, 7102–7108.

(37) Di Bonaventura, G.; Piccolomini, R.; Paludi, D.; D’Orio, V.; Vergara, A.; Conter, M.; Lanieri, A. Influence of temperature on biofilm formation by *Listeria monocytogenes* on various food-contact surfaces: relationship with motility and cell surface hydrophobicity. *J. Appl. Microbiol.* **2008**, *104*, 1552–1561.

(38) Shi, L. L.; Wang, W. L.; Gao, M. N.; Wu, Z. X.; et al. Antibacterial activity and mechanism of action of sulfone derivatives containing 1,3,4-oxadiazole moieties on rice bacterial leaf blight. *Molecules* **2015**, *20*, 11660–11675.

(39) Du, W.; Zhou, M.; Liu, Z.; Chen, Y.; Li, R. Inhibition effects of low concentrations of epigallocatechin gallate on the biofilm formation and hemolytic activity of *Listeria monocytogenes*. *Food Control* **2018**, *85*, 119–126.